Determination of the Raman Polarizability Tensor in the Optically Anistropic Crystal Potassium Dihydrogen Phosphate and Its Deuterated Analog

T. Z. Kosc,[1] H. Huang,[1] T. J. Kessler,[1] R. A. Negres,[2] and S. G. Demos[1]

[1]Laboratory for Laser Energetics, University of Rochester
[2]Lawrence Livermore National Laboratory

Potassium dihydrogen phosphate (KDP) and its deuterated analog (DKDP) crystals are widely used nonlinear optical materials in laser applications. They exhibit excellent UV transmission, high damage thresholds and birefringence, and can be grown to large sizes. These properties make them uniquely suited for use in large-aperture inertial confinement fusion (ICF)–class laser systems such as the OMEGA and OMEGA EP lasers and the National Ignition Facility,[1,2] where they are currently used for frequency conversion,[3] polarization control, and beam smoothing.[4] In large-aperture plates, however, the relatively high Raman scattering cross-section of KDP/DKDP supports the generation and transfer of energy to parasitic beams arising from transverse stimulated Raman scattering (TSRS). This effect is of concern in ICF-class lasers due to the high incident laser intensities and long pulse durations that support the exponential increase of the TSRS signal as it traverses the aperture of the crystal plate[5,6] and ultimately leads, if not properly managed, to damage to the optic and the surrounding hardware during laser operation.[7] The TSRS Raman-gain coefficient can be calculated from the propagation length (optic size), the laser intensity and pulse duration, and a complete description of the spontaneous Raman scattering cross section (Raman polarizability tensor).[8,9] The latter is of critical importance to enable one to model TSRS for suitable crystal-cut configurations to help optimize designs. Theory mandates that the Raman tensor is diagonal,[10] but extensive previous efforts yielded results suggesting contributions by off-axis elements.[11,12] This issue has hindered an accurate modeling of TSRS.

In this work, we determine the form of the Raman tensor and identify artifacts that have interfered in previous studies. A unique experimental system developed at LLE employs spherical samples, which enable one to "directly" measure tensor elements through rotation of the sphere to the required scattering geometries.[13] Data were acquired by rotating the sphere through 360° in the azimuthal plane, which is defined as the laboratory x–z plane and contains both the pump-beam propagation and the Raman signal observation directions (Fig. 1). The azimuthal angle $\phi = 0°$ is defined along the laboratory z axis. Laboratory coordinates are defined by lower-case italicized letters x, y, and z, while upper-case letters X, Y, and Z designate crystallographic axes. The experimental notation k_p [e_p e_s] k_s, designates the propagation direction of the pump k_p, and scattered light k_s as well as the unit electric polarization vectors of the pump e_p and scattered light e_s. For clarity, we define the notation for each trace, or set of measurements while the sample is rotated ($\phi = 0°$ to 360°), based on the initial orientation of the sample for $\phi = 0°$ in reference to the crystal axes. Square brackets are omitted in the trace labels in order to differentiate the notation of a data set and specific Raman scattering configurations within that data set.

Three data sets acquired with the crystallographic Z axis, or the optic axis (OA), found in the azimuthal laboratory x–z plane are shown in Fig. 1. The trace labeled ZYYX provides data for scattering in the Z[YY]X configuration at azimuthal angles $\phi = 0°$ and 180°, while scattering data for the X[YY]Z configuration are collected at $\phi = 90°$ or 270°. The polarization orientations of both the pump laser and the Raman scattering signal (and analyzer) for trace ZYYX are perpendicular to the azimuthal plane. A corresponding trace acquired when (a) the analyzer is rotated by 90° (in the azimuthal plane) is shown as ZYZX, and (b) the pump polarization rotated 90° is shown as ZXYX. The signal of the A_1 mode of KDP,[11] centered at 915 cm^{-1}, is integrated between 860 and 960 cm^{-1}. Unexpected features such as double peaks and valleys are detected at the specific angles of importance for determining the matrix elements.

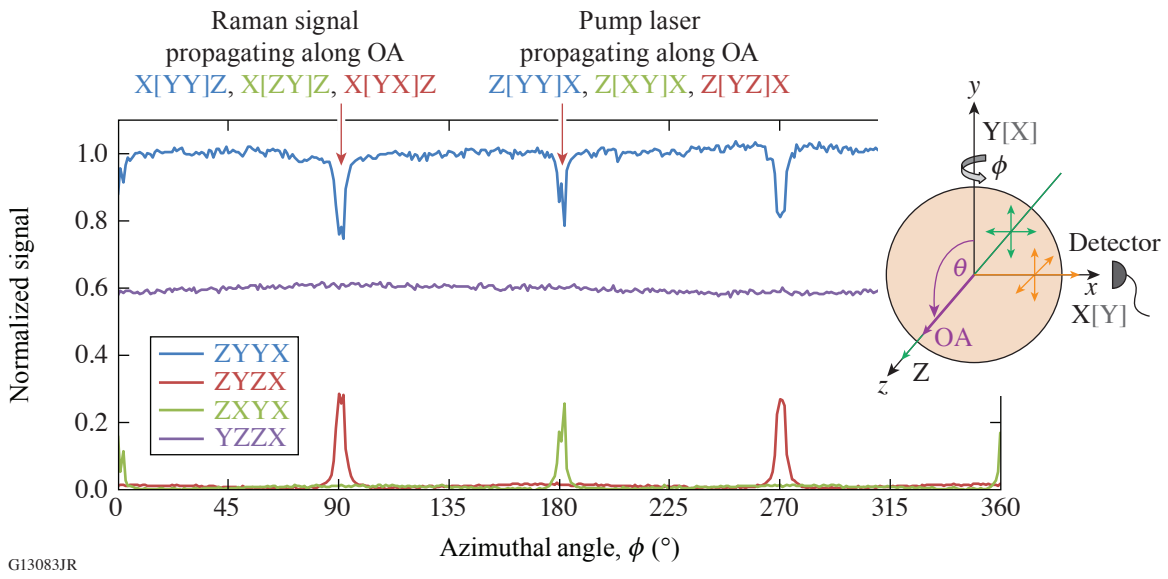

Figure 1
The experimental geometry for Raman scattering measurements is based on a spherical sample (inset). Three traces in which the pump laser and/or the scattering signal propagating along the optic axis experience depolarization are shown. Depolarization artifacts in the form of peaks and valleys arise at azimuthal angles that correspond to configurations at which tensor element values are determined. Data were acquired with an ~1.0° collection half-angle.

These features were reproduced by a ray-trace model that does not consider off-axis tensor elements. The model does consider, however, that in the actual measurement, there is a finite solid angle for the focused laser beam and for the collected Raman scattering. The converging pump laser and the diverging Raman scattering undergo a change of polarization state as a function of propagation length inside the material and orientation of the OA leading to the depolarization of the propagating light. The effect is exacerbated when rays converge or diverge along the OA (because the differential phase between the ray components experiencing the ordinary and extraordinary indices of refraction is the greatest) and increases with the solid angle involved.

Polarization rotation is responsible for the peaks and valleys at critical scattering geometries shown in Fig. 1. The ZYYX trace (blue curve), acquired with the OA lying in the azimuthal plane, should be flat. The polarization, rotation effects observed at $\phi = 0°$ and 180° (Z[YY]X configuration) occur, however, because the vertical polarization of the pump light is altered (i.e., a horizontally polarized component is produced), reducing the amount of Raman signal generated by vertically polarized pump light. An analogous condition exists at $\phi = 90°$ and 270° (X[YY]Z configuration), where the Raman scatter signal propagates along the OA. The Raman scattering signal "lost" to polarization rotation effects appears in configurations for which there should be no Raman scattering from the A_1 mode. Specifically, the slightly wider peaks observed in the ZYZX trace (red) at $\phi = 90°$ and 270° (X[YX]Z configuration) correspond to the polarization rotation of the X[YY]Z configuration exhibiting valleys in the Raman intensity at the same angles. Similarly, the corresponding "lost" signal of the Z[YY]X configuration appears as sharp narrow peaks in the ZXYX trace (green) at the same azimuthal angles (Z[XY]X configuration). Here the polarization rotation of the pump light generates a Z[YY]X component that gives rise to the observed signal where no signal should be found. Note, that data were collected at the smallest-possible collection angle to minimize polarization rotation artifacts.

A closer examination of the Raman scattering spectral profile in the 860- to 960-cm^{-1} integration region for all spectra within each data set led to the identification of additional Raman modes whose spectral profiles partially overlap into the wave number range considered for the determination of the intensity of the 915-cm^{-1} mode. Spectra for the YZZX trace, which includes both Y[ZZ]X and X[ZZ]Y configurations, all show the same strong 915-cm^{-1} peak (Fig. 2). Configurations corresponding to the ZYXY trace, Z[YX]Y and Y[ZX]Z, determine off-axis tensor elements and should not generate a scattering signal. Spectral analysis confirmed that the strong peaks at $\phi = 0°$ and 180° in the ZYYX trace are due to a 915-cm^{-1} peak arising from depolarization effects. The spectrum for the X[ZY]Z configuration reveals that Raman scattering from additional low-intensity modes adjacent

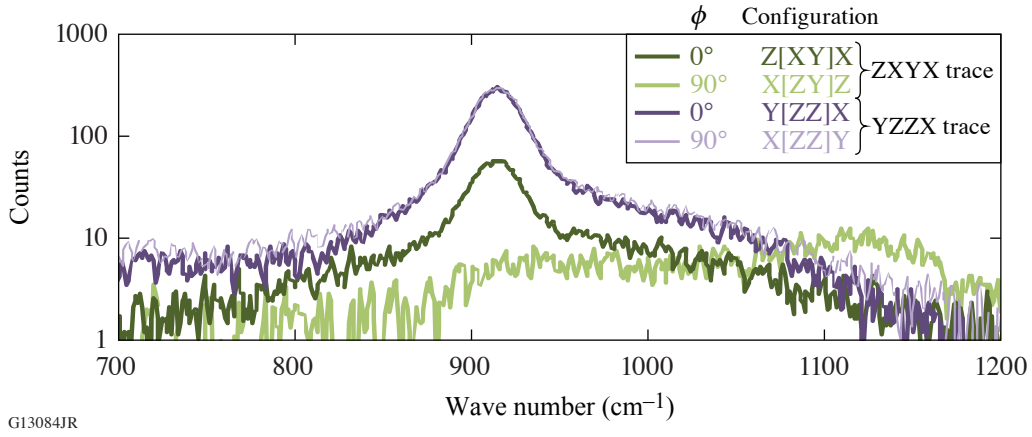

Figure 2
Selected spectra at 0° and 90° demonstrate the presence of Raman scattering from the dominant A_1 mode of KDP (trace YZZX) and the depolarization and the overlap of neighboring modes (trace ZXYX). Data acquired with an ~0.5° focusing half-angle and 1.0° collection half-angle.

to the 915-cm^{-1} mode overlap with the integration region and give rise to erroneous signals that can be misinterpreted as arising from nondiagonal matrix elements.

The theoretical description of the Raman tensor R for the A_1 mode is represented by a diagonal matrix.[13] In the following analysis, all other tensor elements are normalized to the value of A, which is assigned the maximum value of trace ZYYX (or ZXXY). The matrix element B is determined solely by averaging of the entire trace YZZX. The examination of spectra for all experimental configurations confirmed that the Raman tensor for the dominant A_1 mode contains no off-axis terms. The same analysis was performed for both KDP and 70% DKDP samples tested in an experimental setup using a 1.0° collection half-angle. Future work will explore the dependence of the collection aperture on the tensor element values more carefully.

$$R(\mathrm{A_1}) = \begin{pmatrix} A & 0 & 0 \\ 0 & A & 0 \\ 0 & 0 & B \end{pmatrix} \quad R_{\mathrm{KDP}} = \begin{pmatrix} 1 & 0 & 0 \\ 0 & 1 & 0 \\ 0 & 0 & 0.79 \pm 0.01 \end{pmatrix} \quad R_{70\%\ \mathrm{DKDP}} = \begin{pmatrix} 1 & 0 & 0 \\ 0 & 1 & 0 \\ 0 & 0 & 0.76 \pm 0.02 \end{pmatrix}.$$

This material is based upon work supported by the Department of Energy National Nuclear Security Administration under Award Number DE-NA0003856, the University of Rochester, and the New York State Energy Research and Development Authority.

1. J. D. Lindl *et al.*, Phys. Plasmas **11**, 339 (2004).
2. N. Fleurot, C. Cavailler, and J. L. Bourgade, Fusion Eng. Des. **74**, 147 (2005).
3. W. Seka *et al.*, Opt. Commun. **34**, 469 (1980).
4. T. R. Boehly *et al.*, J. Appl. Phys. **85**, 3444 (1999).
5. C. E. Barker *et al.*, Proc. SPIE **2633**, 501 (1995).
6. S. N. Dixit *et al.*, J. Phys. IV France **133**, 717 (2005).
7. K. R. Manes *et al.*, Fusion Sci. Technol. **69**, 146 (2016).

8. Y. R. Shen and N. Bloembergen, Phys. Rev. **137**, A1787 (1965).

9. A. Z. Grasiuk and I. G. Zubarev, Appl. Phys. **17**, 211 (1978).

10. R. Loudon, Adv. Phys. **13**, 423 (1964).

11. W. L. Smith, M. A. Henesian, and F. P. Milanovich, *Laser Program Annual Report 1983*, 6-61, Lawrence Livermore National Laboratory, Livermore, CA, Report UCRL-50021-83 (1984).

12. S. G. Demos *et al.*, Opt. Express **19**, 21050 (2011).

13. T. Z. Kosc *et al.*, Rev. Sci. Instrum. **91**, 015101 (2020).